Journal of Solid State Chemistry **144,** 45–52 (1999)
Article ID jssc.1998.8115, available online at http://www.idealibrary.com on IDEAL®

Acidic and Hydrophobic Microporous Clays Pillared with Mixed Metal Oxide Nano-Sols

Yang-Su Han,* Shoji Yamanaka,† Jin-Ho Choy*,[1]

*Department of Chemistry, Center for Molecular Catalysis, Seoul National University, San56-1, Shilim-dong, Kwanak-gu, Seoul 151-742, Korea; and †Department of Applied Chemistry, Faculty of Engineering, Hiroshima University, Higashi–Hiroshima 739, Japan

Received April 2, 1998; in revised form November 17, 1998; accepted November 27, 1998

Silica–metal oxide sol pillared clays have been synthesized from montmorillonite by exchanging interlamellar (Na^+) ions with silica sol particles modified with polyhydroxy metal cations. Though the silica sol particle itself is negatively charged in the pH range used in present experiment, 1.5–2.7, the ion-exchange-type intercalation of the silica sol into montmorillonite was realized by modifying the surface charge of the sol particles from negative to positive. The positively charged silica sol particles were prepared by titrating metal aqueous solutions (M^{z+} = Fe^{3+}, Al^{3+}, Cr^{3+}, and Zr^{4+}) with NaOH in the presence of silica sol particles, which were easily intercalated inbetween the silicate layers of clay. On pillaring of oxide sols and subsequent calcining at 400°C, new porous materials were obtained with high BET surface areas of 320–720 m^2/g, pore volumes of 0.24–0.50 ml/g, and basal spacings in the range 40–60 Å. Furthermore, their thermal stability could be remarkably improved up to 700°C. According to the adsorption measurements of nitrogen and solvent vapors, the micropores in the samples of size 9–13 Å dominate due to the multilayer stacking of interlayer sol particles inbetween silicate layers. Temperature-programmed desorption (TPD) spectra of ammonia revealed that the microporous samples are weakly acidic, but with different strengths, depending on the doped metal species.

INTRODUCTION

In an attempt to improve the limited pore size range in which zeolites are available, there has been renewed interest in the preparation of novel, two-dimensional, molecular sieve-type materials based on clays, called pillared interlayer clays (PILCs) (1–3). PILCs have received much attention as a new type of microporous solid that can serve as shape-selective catalysts, catalytic supports, separating agents, adsorbents, etc. In particular, clays pillared by metal oxides are of great interest because of their high surface area and intrinsic catalytic activity.

[1]To whom correspondence should be addressed. Fax: 82-2-872-9864. E-mail: jhchoy@plaza.snu.ac.kr.

Conventionally, these microporous materials are obtained by exchanging the interlayer cations of clays with bulky inorganic cations followed by calcination. On heating, the intercalated cations are converted to metal oxide clusters, propping open the layers as pillars, generating interlayer space of molecular dimensions, i.e., a two-dimensional porous network. Because the micropore structure, thermal stability, and intrinsic catalytic activity of such prepared PILCs are greatly influenced by the nature of the pillar, various kinds of pillar, including metal polycations such as Al, Zr, Cr, Ti, Si, Fe, and Ga (4–15), mixed metal cluster cations such as Al–Si, Al–Zr, Al–La,Ce, and Al–Fe,Cr (16–19), and positively charged colloidal sol particles like TiO_2, Al_2O_3, SiO_2–Al_2O_3, SiO_2–TiO_2, and SiO_2–Fe_2O_3 (20–25) have been introduced into two-dimensional silicate layers to obtain tailormade PILCs for specific applications.

Among many potential applications of PILCs, the use of PILCs as catalysts has attracted considerable attention due to their intrinsic catalytic activity and molecular sieving function. It has been reported that pillared clays have a cracking activity comparable to that of zeolites (2, 3). Moreover, PILCs with larger pores can admit larger hydrocarbons. However, high thermal or hydrothermal stability of the materials is required, especially during regeneration of deactivated catalyst. Unfortunately, the pillared clays developed to date do not have sufficient thermal stability. To overcome such a problem, several attempts have been made to introduce mixed metal oxide pillars (16–19), by pretreating the pillar species hydrothermally (26) and by applying thermally stable aluminosilicates like rectorite (27, 28).

In previous work (24), the negative surface charge of silica sol could be modified by depositing positively charged TiO_2 sol particles, which could be intercalated successfully between the silicate layers to form pillared clays with high surface area and relatively good thermal stability. Recently, we have also found that silica sols can be modified with metal polyhydroxy cations (M^{z+}) such as Fe, Cr, Al, and Zr,

0022-4596/99 $30.00

which are incorporated into the silicate layers as pillars to form highly porous sol pillared clays of high thermal stability (25). The primary objectives of this study are to prepare the silica-based mixed sol particle pillared clays, to characterize their adsorption properties, and also to investigate the effects of positive metal species (M^{z+}) on the internal pore structure, thermal stability, and acidic property of sol pillared clays.

EXPERIMENTAL

1. Preparation of Sol Pillared Clay

A natural Na-montmorillonite (Kunipia G) with structural formula $Na_{0.35}K_{0.01}Ca_{0.02}(Si_{3.89}Al_{0.11})(Al_{1.60}Mg_{0.32}Fe_{0.08})O_{10}(OH)_2 \cdot nH_2O$ and cation-exchange capacity (CEC) 100 meq/100 g was used as starting material. Five grams montmorillonite was dispersed in 500 ml deionized water and swelled for 1 day prior to the reaction with sol solutions.

A silica sol solution was prepared as previously reported (24,25) by mixing silicon tetraethoxide (TEOS, $Si(OC_2H_5)_4$), 2 *N* HCl, and ethanol in the ratio 41.6 g/10 ml/12 ml and further by peptizing at room temperature for 2 h. Each metal aqueous solution of 1.0 M was prepared by dissolving $Fe(NO_3)_3 \cdot 9H_2O$, $Al(NO_3)_3 \cdot 9H_2O$, $Cr(NO_3)_3 \cdot 6H_2O$, and $ZrOCl_2 \cdot 8H_2O$ in deionized water, respectively. Then the aqueous solutions were added to the silica sol solution, followed by the base titration with 0.2 N NaOH solution. During the titration, the pH of mixed solutions was adjusted to the desired values—2.7 for Fe^{3+}, 2.5 for Al^{3+}, 2.1 for Cr^{3+}, and 1.5 for Zr^{4+}—to facilitate the oligomerization of metal species on the silica sol surfaces and to avoid undesirable precipitation. In the cases of Al- and Cr-containing mixed sol solutions, further oligomerization was carried out at 80°C for 1 h prior to the ion-exchange reaction. The mixed sol solutions thus prepared were mixed with the clay suspension in the molar ratio of $Si/M^{z+}/CEC = 50/5/1$. Then the mixture was reacted for 3 h under stirring at 60°C except for the SiO_2–ZrO_2 system, which was made at room temperature for 12 h. The reaction products were separated by centrifuging, washed with a mixed solution of ethanol and water (1:1 v/v) several times to remove the excess sol solutions, and then dried in air. Finally, the samples were calcined for 2 h in the temperature range 200 ~ 800°C under an ambient atmosphere. The SiO_2–Fe_2O_3, SiO_2–Al_2O_3, SiO_2–Cr_2O_3, and SiO_2–ZrO_2 pillared montmorillonites produced are abbreviated hereafter as SFM, SAM, SCM, and SZM, respectively.

2. Characterization

Powder X-ray diffraction patterns were obtained for the oriented samples using a diffractometer (SRA-M18XHF, MAC Science Co.) with graphite monochromatized Cu$K\alpha$ radiation ($\lambda = 1.5418$ Å). The oriented samples were prepared by spreading a small portion of wet samples on a quartz glass slide before calcination. Thermogravimetry (TG) analyses were performed with a Seiko 8071E1 thermobalance by heating 50 mg at 5°C min^{-1} from 25 to 800°C under an oxygen and nitrogen mixture gas stream with a 1:1 volume ratio (flow rate: 100 ml/min). Elemental analyses of the pillared products were carried out by inductively coupled plasma (ICP; Perkin Elmer Optima 3000), for which the samples were fused with lithium metaborate at 900°C and dissolved in 3% HNO_3 solution.

Nitrogen adsorption–desorption isotherms were measured volumetrically at the liquid nitrogen temperature with a computer-controlled measurement system. The samples were degassed at 200°C for 3 h under a reduced atmosphere prior to the sorption measurement. Specific surface areas of the pillared samples were estimated from both BET and Langmuir equations. Micropore volumes (V_{micro}) and surface areas (S_{micro}) were calculated based on the *t*-plot method of nitrogen (29). A *t* curve for nonporous silica was used as a standard. Pore size distribution was calculated from the adsorption branches by applying the micropore analysis (MP) method (30). Adsorption–desorption isotherms for some selected solvent vapors of different molecular sizes were measured gravimetrically at 25°C with a Cahn balance. The pillared samples were also degassed at 200°C for 3 h prior to the sorption measurement.

To characterize the acidic property of the sol pillared clays, temperature-programmed desorption (TPD) spectra of ammonia were recorded for the samples calcined at 600°C by gas chromatography with a thermal conductivity detector. About 200 mg of the sample was reheated at 400°C for 1 h in a stream of helium and cooled to room temperature and exposed to ammonia vapor ($P_{NH_3} = 1$ atm) for 30 min, and the excess ammonia was purged with a flow of helium at room temperature for 5 h. The measurement was carried out up to 550°C with a heating rate of 5°C/min and a helium flow rate of 100 ml/min. TPD spectra of ammonia for H-ZSM-5 were also recorded to compare the acidic nature.

RESULTS

1. Pillaring of Mixed Metal Oxide Sols

Since the surface of the SiO_2 sol particle is negatively charged in an acidic aqueous solution, it is necessary to modify the surface charge positively for incorporation into the negatively charged clay lattices. It was reported that addition of a small amount of titania sol to silica sol solution is sufficient to modify the surface charge of silica, leading to intercalation of SiO_2 sol into clay (24). The metal cations used in this study also form various types of polyhydroxy cations in an acidic aqueous solution. The resulting polyhydroxy cations would be easily deposited on the negatively charged silica surface, giving rise to the positive silica sol particles.

2. X-ray Diffraction Patterns

The mixed sol particles with a positive surface charge can easily be intercalated into clay lattices as represented in Fig. 1. The basal spacings of the samples calcined at 400°C are in the range 40–58 Å, suggesting the formation of "super-gallery" pillared clays in which the gallery height is substantially larger than the thickness of clay layers (~10 Å). In the cases of SFM (a) and SZM (d), higher order reflection profiles (at least second order) are clearly observed and are indicative of the regular stacking of sol pillared layers. The diffraction peaks of SAM (b) and SCM (c) exhibit relatively broad (001) reflections centered at 57 and 47 Å, respectively, indicating that the interlayer sol particles are stacked rather irregularly.

The evolution of basal spacings of sol pillared clays is plotted with respect to calcination temperature (Fig. 2). The basal spacings are almost constant up to 500°C, even though a slight decrease is observed depending on the pillar. All the samples exhibit somewhat drastic changes in basal spacings in the temperature range 500–600°C, which is due not only to the dehydroxylation of silicate lattices, but also to the contraction of interlayer sol pillars. Even after calcination at 800°C, the fairly large basal spacings of 35–50 Å are maintained, implying that the regularity of the two-dimensional structures generated on pillaring of sol particles is fairly well retained up to this temperature.

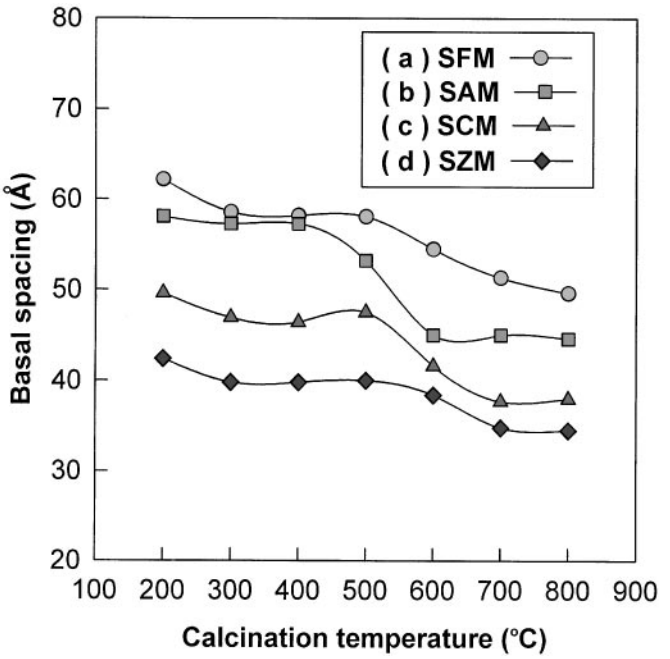

FIG. 2. Basal spacings of sol pillared clays as a function of calcination temperature.

3. Thermal Analysis

The TG curves of the air-dried sol pillared samples are shown in Fig. 3. The first step below 200°C can be attributed to the loss of physisorbed water and loosely coordinated water. The second step with continuous weight losses up to

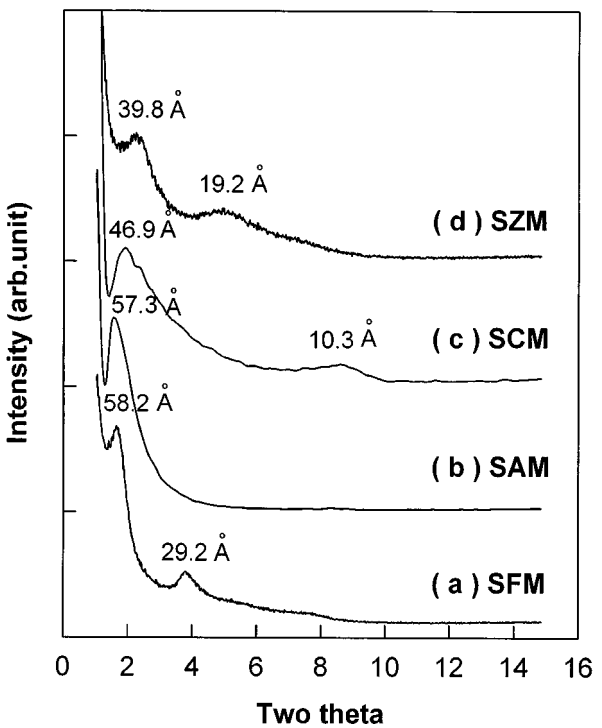

FIG. 1. X-ray diffraction patterns of mixed oxide sol pillared clays calcined at 400°C for 2 h: (a) SFM, (b) SAM, (c) SCM, (d) SZM.

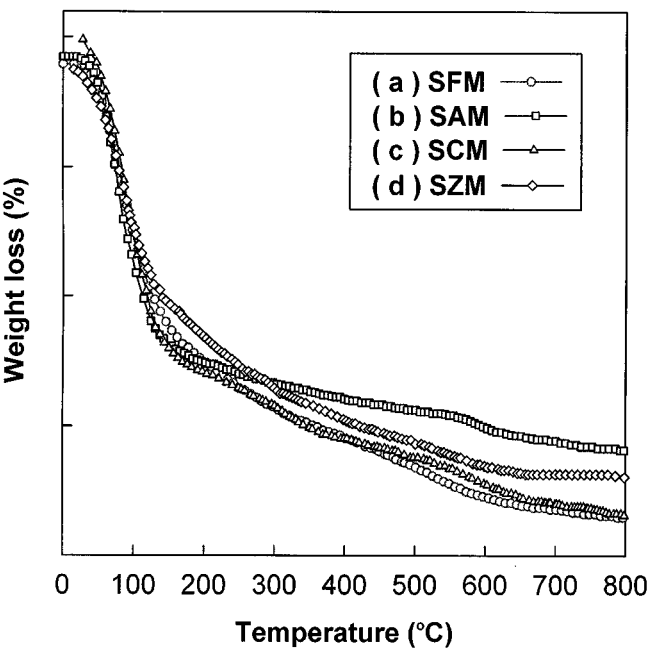

FIG. 3. Thermogravimetry curves of air-dried sol pillared samples under an ambient atmosphere: (a) SFM, (b) SAM, (c) SCM, (d) SZM.

about 500°C is due to the dehydroxylation of OH groups associated with interlayer pillars. And an additional weight loss at around 600°C can be assigned to the dehydroxylation of silicate layers in the clays (31, 32).

4. Chemical Analysis

To evaluate the chemical composition of mixed oxide sol particles intercalated, the pillared products were analyzed by the ICP method as summarized in Table 1. Under the assumption that the composition of starting Na-montmorillonite is constant throughout the pillaring process, the structural formula of the pillared products could be determined. In the calculation, the amounts of SiO_2, Fe_2O_3, and Al_2O_3 coming from silicate layer itself were systematically excluded. The resulting sol formula, $(SiO_2)_x(MO)_y$, is shown on the $O_{10}(OH)_2$ anion basis of the clay. The pillar compositions are strongly dependent on the kinds of positive metal species due to their different degrees of hydrolysis in an aqueous solution and on the strength of interaction between metal ion species and silica surface.

5. Nitrogen Adsorption–Desorption Isotherms

Figure 4 presents the nitrogen adsorption–desorption isotherms of sol pillared samples calcined at 400°C for 2 h. All the adsorption isotherms can be classified as Type I according to the BDDT classification (29) at low relative pressure, indicating that the pores formed in the sol pillared clays are much smaller than the interlayer separations. On the other hand, they exhibit hysteresis during desorption at higher P/P_0, due to the adsorption in the mesopores which are derived mainly from the "house of cards" structure of clay particles (29). The adsorption isotherms give a good fit to the Langmuir equation (Type I) as well as the BET equation (infinite number of adsorption layers), even though a better fit is obtained with the BET equation for the limited number of nitrogen adsorption layers. Only the adsorption isotherm for SZM gives a better fit with the Langmuir equation, suggesting that monolayer nitrogen adsorption takes place due to restricted pore dimensions.

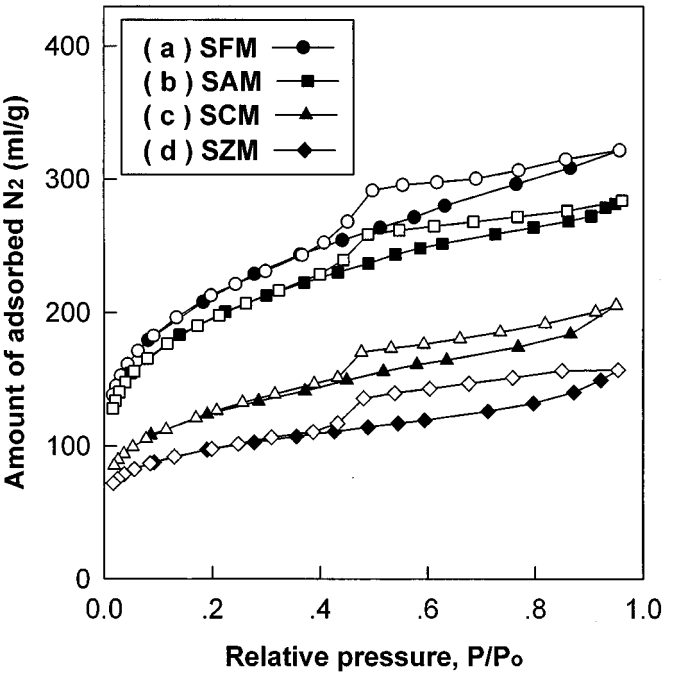

FIG. 4. Nitrogen adsorption–desorption isotherms of mixed oxide sol pillared clays calcined at 400°C for 2 h: (a) SFM, (b) SAM, (c) SCM, (d) SZM.

The pore parameters calculated from nitrogen adsorption–desorption isotherms are summarized in Table 2. It is found that high BET surface areas of 320–720 m^2/g and pore volumes in the range 0.24–0.50 ml/g originate mainly from micropores. In addition, it is worthy to note here that the sol pillared clays show excellent thermal stability. To compare quantitatively, we introduced arbitrarily a critical stability temperature (CST) defined as the maximum heating temperature at which the surface area is maintained more than 60% compared with the maximum one. In the cases of SFM, SAM and SCM, more than 60% of the

TABLE 1
Chemical Analysis Data for Mixed Metal Oxide Sol Pillared Clays

Pillared sample	Analytical results (mol%)						Pillar compositions[a]		
	SiO_2	Fe_2O_3	Al_2O_3	Cr_2O_3	ZrO_2	MgO	$(SiO_2)_x$	$(MO)_y$	$x + y$
SFM	76.0	11.2	10.8	—	—	—	8.19	0.90	9.09
SAM	75.3	—	21.1	—	—	1.96	8.41	0.87	9.28
SCM	84.1	—	9.3	4.1	—	—	11.6	0.38	12.0
SZM	77.4	—	13.1	—	6.5	—	6.24	0.84	7.08

[a]The pillar compositions (x and y) are given in moles of $[(SiO_2)_x(MO)_y][(Si_{3.89}Al_{0.11})(Al_{1.60}Mg_{0.32}Fe_{0.08})]O_{10}(OH)_2$ formula, where $MO = Fe_2O_3$, Al_2O_3, Cr_2O_3, and ZrO_2.

TABLE 2
Specific Surface Areas and Pore Volumes of Sol Pillared Clays Calcined at 400°C for 2 h and Critical Stability Temperatures

Pillared sample	Surface Area (m^2/g)		Pore volume (ml/g)		Critical stability temperature[b] (°C)
	BET	S_{micro}-[a]	Total	V_{micro}-[a]	
SFM	722	468	0.50	0.27	700
SAM	654	472	0.44	0.27	700
SCM	412	267	0.32	0.15	700
SZM	317	203	0.24	0.11	500

[a]Estimated by t-plot method (29).

[b]Temperature at which the surface area is maintained more than 60% compared with the maximum one of the sample.

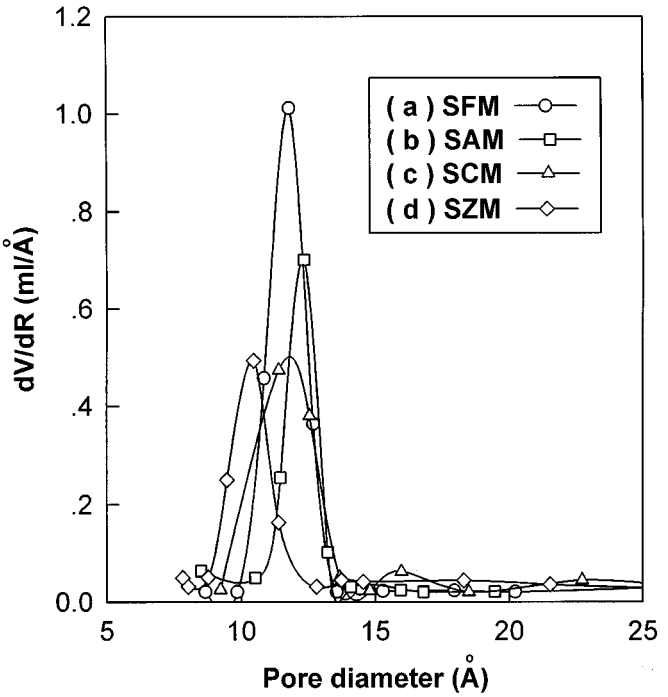

FIG. 5. Pore volume distribution curves of sol pillared clays calcined at 400°C for 2 h; (a) SFM, (b) SAM, (c) SCM, (d) SZM.

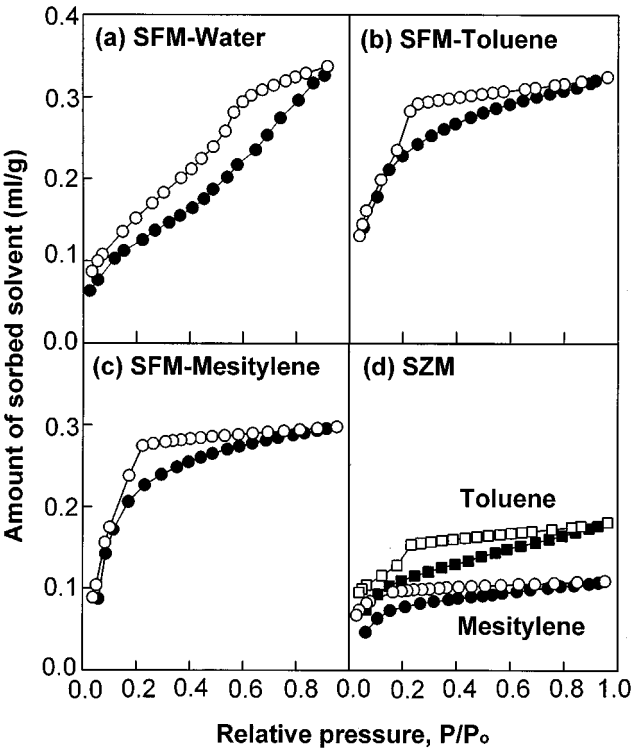

FIG. 6. Solvent adsorption–desorption isotherms for SFM [(a) water, (b) toluene, (c) mesitylene] and SZM [(d) toluene and mesitylene].

maximum surface area is maintained even after calcining at 700°C, indicating the micropores generated between sol particles are quite stable. The microporous structures of these samples seem to collapse between 700 and 800°C. On the other hand, SZM reveals comparatively low thermal stability with a CST of 600°C.

Using the adsorption branches in Fig. 4, the pore size distribution could be estimated by applying the MP method (30) as plotted in Fig. 5. Despite the large basal spacings, the pore volume increases mainly in the part of micropore (<20 Å) range of 9–13 Å.

6. *Solvent Adsorption Isotherms*

Adsorption–desorption isotherms for some kinds of solvents vapors of different molecular size are measured at 25°C. The isotherms for water, toluene, and mesitylene of SFM are presented in Figs. 6a–6c, and those of SZM in Fig. 6d, respectively. The adsorption isotherms for large molecules such as toluene and mesitylene fit well the Langmuir linear plot, whereas those for smaller molecules (water) fit the BET equation. This finding suggests that the pore size is on the order of the largest molecular size examined in the present study (~7.6 Å for mesitylene). This is also in good agreement with the fact that the nitrogen adsorption isotherm fits the BET plot for a limited number of adsorption layers.

Typically it has been well known that water adsorption on pillar surface is suppressed due to the hydrophobic nature of the oxide pillar surface (33), as also found in the present water adsorption study on SiO_2–Fe_2O_3 sol pillared clay. Similar adsorption behavior is observed for other sol pillared samples. The hysteresis of desorption branch extending to very low P/P_0 in toluene and mesitylene isotherms is associated with the "activated entry" of large adsorbate molecules through fine pores (34).

According to the adsorption–desorption isotherms of toluene and mesitylene for the SZM sample (Fig. 6d), the amount of toluene adsorbed is twice larger than that of mesitylene, suggesting that the pore size is on the order of the molecular size of toluene (~ 6 Å). This is also well consistent with the finding that the nitrogen adsorption isotherm fits well the Langmuir equation for a monolayer adsorption rather than the BET equation.

7. *TPD Spectra of Ammonia*

The TPD spectra of ammonia for mixed oxide sol pillared clays calcined at 600°C are presented in Fig. 7. The ammonia desorption spectrum of H-ZSM-5 is also overlain for comparison. According to the previous literature (1–3), the pillared clays contain both Brønsted and Lewis acidic sites. However, the former disappears rapidly when the pretreatment temperature is higher than 400°C, which is

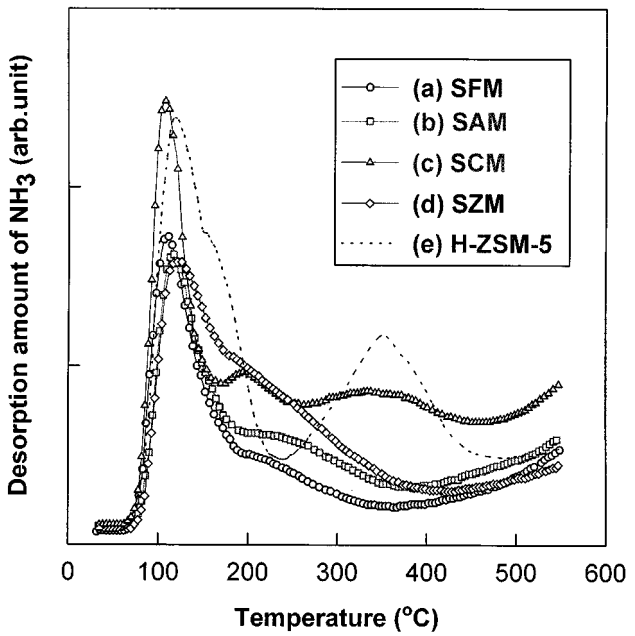

FIG. 7. Temperature-programmed-desorption spectra of ammonia for sol pillared clays calcined at 600°C: (a) SFM, (b) SAM, (c) SCM, (d) SZM, (e) H-ZSM-5.

often attributed to a migration of protons on heating from the interlayer space into the octahedral layer, where they neutralize the negative layer charge. Thus, the desorption peaks observed in Fig. 7 are associated mainly with Lewis rather than Brønsted acid centers. In Fig. 7, the strong desorption peaks near 100°C can be assigned to the desorption of ammonia loosely bound to weak acidic sites or, in part, to the surface-adsorbed water. The following weak desorption peaks in the temperature range 200–350°C are somewhat different in position and intensity according to the samples, implying that the acidic nature of MO–SiO_2 sol pillared clays is dependent on the MO species on silica sol surfaces, which provides a new way of controlling the surface acidity of pillared clays. Compared with H-ZSM-5, the present mixed oxide sol pillared clays can be characterized as weak acidic solids. In the case of SCM (c), an additional desorption peak centered at 360°C is observed due to the dissociation of ammonia from strong acidic centers. Though the exact origin for this has not been fully understood yet, it is likely that the strong acidic sites come from the additional Cr_2O_3 pillared phase (Fig. 1c, a weak reflection at 10.3 Å), exhibiting a higher ammonia desorption peak than that of Al (320°C) (35).

DISCUSSION

1. Formation of Mixed Metal Oxide Sol Particles

The results discussed above strongly suggest that the most important step to mixed oxide sol pillared clay is the formation of well-developed mixed oxide sols before ion-exchange reaction. Thus, the control of suitable preparation conditions for mixed oxide sol solution is highly critical. The metal cations used in this study form various types of polyhydroxy cations depending on solution parameters such as pH, concentration, temperature, kinds of counter-anions, and aging condition. With an increase in pH, temperature, and aging time, the hydrolysis reaction becomes favorable, leading to an increase in the degree of polymerization, the basal spacing, and eventually the surface area of the pillared clay.

As reported previously (36, 37), the dissolution of iron salts in water results initially in simple hydrolysis products [$FeOH^{2+}$, $Fe(OH)_2^+$, $Fe_3(OH)_4^{5+}$, etc.], and further hydrolysis in the pH range 2–3 leads to the formation of moderately polymerized iron species [$Fe_x(OH)_y^{z+}$]. Since the surface of silica particles has a negative charge in this pH range, the Fe^{3+} ions are deposited onto the silica surface and then grow to polycation species by base titration. Such modified silica sol particles have enough of a positive surface charge to be intercalated between silicate layers and seem quite uniform in size as reflected in a higher-order X-ray diffraction pattern (Fig. 1a), which is due to the regular stacking of interlayer sol particles of uniform size between the layers.

From the aqueous chemistry of Al^{3+}, highly polymerized species of $Al_{13}O_4(OH)_{24}(H_2O)_{12}^{7+}$, which is usually used to prepare the Al_2O_3 pillared clays, can be prepared by adjusting the solution pH to 4 with extended aging (38). In the presence of silica sols, however, an increase in pH above 3 or further hydrolysis leads to undesirable aluminosilicate gel precipitation. Thus, the solution pH should be controlled carefully to prevent undesirable precipitation and to facilitate the oligomeriztion of Al species as well. Even though the preparation conditions (pH $\sim$ 2.5 and 80°C for 1 h) used in this work are not sufficient to obtain highly polymerized species, some dimeric [$Al_2(OH)_2^{4+}$] or trimeric [$Al_3(OH)_4^{5+}$] complexes might be formed on silica surfaces to modify the surface charge from negative to positive. The sol particles prepared, however, seem to have broader size distribution as demonstrated in a broader X-ray diffraction profile with an absence of long range ordering (Fig. 1b).

Small chromium oligomers, including dimers, trimers, and tetramers, have been identified and isolated from solutions at various pH values (10). The hydrolysis rates even for small chromium oligomers are known to be exceptionally low (35), and therefore, the hydrolysis rate was accelerated by adding bases or aging at higher solution temperature, but this often gives rise to unavoidable gel precipitation in the presence of silica sol solution. In the present study, the proper conditions for the formation of Cr-coated silica particles without gel precipitation were found to be a solution pH of 3 and an aging temperature of 80°C (for 1 h). Even under these conditions, however, the formation of uniform Cr-coated silica particles is not always successful as

shown in Fig. 1c, where only a broad (001) reflection can be seen, indicating lower regularity of interlayer mixed sol particles.

The dissolution of Zr(IV) salts in water is known to result initially in tetrameric $Zr_4(OH)_8^{8+}$. Further hydrolysis leads to formation of a tetramer with the formula $Zr_4(OH)_{14}^{2+}$ and eventually results in the precipitation of hydrous $Zr(OH)_4$ in the pH range 2–2.5 (38). In the presence of silica sol solution, however, the conditions for enhancing polymerization cannot be applicable directly due to the unavoidable gel precipitation. Since the pH (1.5) used in the present study is not sufficient to obtain highly polymerized Zr species, the size of mixed sol particles and the amount of intercalated sols are probably small, which results in shorter basal spacings with lower specific surface areas. The tetrameric species, $Zr_4(OH)_8^{8+}$, exists solely in this pH domain without any disturbance from other polymeric species, and therefore, the Zr-coated silica particles must be uniform in size. It is apparent from XRD result (Fig. 1d), suggesting well ordered stacking of interlayer sol particles.

2. *Structure of Oxide Sol Pillared Clays*

As shown in Fig. 1, the resulting pillared clays have basal spacings remarkably larger than those reported so far for pillars with metal oxides. It is therefore assumed that the large sol particles, corresponding to the pillar heights or the multilayer stacking of small sol particles, are incorporated into the interlayers of clay as previously reported (24,25). However, the adsorption data exclude the possibility of the former since most of the pores obtained are much smaller than the interlayer distance. Therefore it is reasonable to assume multilayer stacking of small sol particles where micropores are formed among sol particles and silicate layers as represented schematically in Fig. 8.

3. *Thermal Stability of Oxide Sol Pillared Clays*

Mixed oxide sol pillared clays of high porosity exhibit excellent thermal stability, which is determined by the structural stability of silicate lattices and pillar species (3). Although decomposition of the structural OH groups in the dioctahedral smectites occurs at around 600°C (Fig. 3), the framework of the silicate layer can be made stable at higher temperatures (~800°C) if the structural OH groups are converted to O^{2-} ion by condensation with oxides or hydroxides between the silicate layers (31, 32). Then, collapse of the pillared structure is attributed mainly to the sintering of pillars and a total reaction between pillars and silicate layers. In the present pillared clays, the formation of strong covalent bonds between sol particles and the tetrahedral layer of montmorillonite is primarily responsible for high temperature stability, as is often observed in conventional pillared clays (2, 3, 31, 32). In addition, a regular multistacking of interlayer sol particles with high sintering resistance increases the density of pillars within the interlayer space, providing a high contact area with clay sheets, which gives stability to the pillared structure.

It is well known that Cr-containing pillared clays are poor in thermal stability mainly due to the air oxidation of Cr^{3+} to a more mobile Cr species like Cr^{6+} (35). Although we cannot provide straightforward evidence of the enhanced thermal stability of SiO_2–Cr_2O_3 sol pillared clay, it is likely that the silica sol particles act mainly as strong pillars to keep silicate layers apart. Moreover, Cr species supported by silica particles seem to have an enhanced oxidation resistance.

In the case of SZM, a substantially large interlayer separation (~25 Å) was observed even after calcining at 800°C (Fig. 2), while the microporous structure characterized by N_2 adsorption almost collapsed after heating above 600°C (Table 2). As illustrated in Figs. 4–6, SZM has a comparatively smaller pore size than the others. Thus, partial sintering of pillars on heating may have a great influence on the pore narrowing or blocking, which makes the adsorbate molecules inaccessible to the pores due to the limited pore size. However, the sintered sol particles still remain quite ordered to some extent up to higher temperature, giving rise to a distinct X-ray diffraction peak (Fig. 1d).

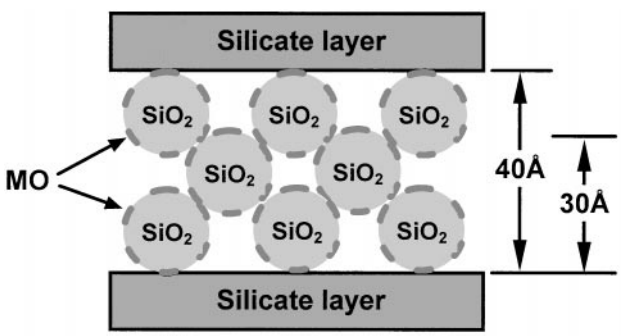

FIG. 8. Schematic structural model for mixed metal oxide sol particle pillared clays.

CONCLUSIONS

New mixed metal oxide sol pillared clays were prepared successfully by ion exchange of Na^+ ions in montmorillonite with SiO_2–MO ($MO = Fe_2O_3, Al_2O_3, Cr_2O_3, ZrO_2$) sol particles. The oxide sol pillared clays exhibited remarkably high BET surface areas (320–720 m^2/g), pore volumes (0.24–0.50 ml/g), basal spacing (40–60 Å), and excellent thermal stability up to 700°C. According to the adsorption data on nitrogen and solvent vapors, the pores formed are hydrophobic and mostly micropores of 9–13 Å. Based on these findings, a model for multilayer stacked interlayer sol particles is proposed where the interstices among sol particles and silicate layers act as micropores. Finally, TPD

revealed that the microporous solids are weakly Lewis acidic with different strengths depending on the pillar.

ACKNOWLEDGMENTS

This work was supported by KOSEF (Korea Science and Engineering Foundation) through the Center for Molecular Catalysis. Y. S. Han is grateful for the fellowship under the program of Korea–Japan Researchers' Friendship.

REFERENCES

1. K. Ohtsuka, *Chem. Mater*. **9,** 2039 (1997).
2. R. Burch (Ed.), "Pillared Clays," Spec. Publ. *Catal. Today* **2** (1988).
3. F. Figuers, *Catal. Rev. Sci. Eng*. **30,** 457 (1988).
4. L. Bergaoui, J. F. Lambert, M. A. Vicente-Rodriguez, L. J. Michot, and F. Villieras, *Langmuir* **11,** 2849 (1995).
5. L. Bergaoui, J. F. Lambert, R. Franck, H. Suquet, and J.-L. Robert, *J. Chem. Soc. Faraday Trans*. **91,** 2229 (1995).
6. G. W. Brindley and R. E. Sempels, *Clay Miner*. **12,** 229 (1977).
7. N. Lahav, U. Shani, and T. Shabtai, *Clays Clay Miner*. **26,** 107 (1978).
8. K. Ohtsuka, Y. Hayashi, and M. Suda, *Chem. Mater*. **5,** 1823 (1993).
9. T. J. Pinnavaia, M. S. Tzou, and S. D. Landau, *J. Am. Chem. Soc*. **107,** 4783 (1985).
10. A. Drljaca, J. R. Anderson, and T. W. Turney, *Inorg. Chem.* **31,** 4894 (1992).
11. A. Bernier, L. Admaiai, and P. Grange, *Appl. Catal.* **77,** 269 (1991).
12. R. M. Lewis, K. C. Ott, and R. A. Van Santen, *U.S. Patent* 4,510,257 (1985).
13. E. G. Rightor, M. S. Tzou, and T. J. Pinnavaia, *J. Catal*. **130,** 29 (1991).
14. S. M. Bradley and R. A. Kydd, *J. Chem. Soc. Dalton Trans*., 2407 (1993).
15. S. Yamanaka and G. W. Brindley, *Clays Clay Miner*. **27,** 119 (1979).
16. J. Sterte and J. Shabtai, *Clays Clay Miner*. **35,** 429 (1987).
17. X. Tang, W. Q. Xu, Y. F. Shen, and S. L. Suib, *Chem. Mater*. **7,** 102 (1995).
18. E. Booij, T. Kloprogge, and J. A. Rob van Veen, *Clays Clay Miner*. **44,** 774 (1996).
19. I. Pálinkó, A. Monlár, J. B. Nagy, J.-C. Bertrand, K. Lázár, and J. Valyon, *J. Chem. Soc. Faraday Trans*. **93,** 1591 (1997).
20. S. Yamanaka, T. Nishihara, M. Hattori, and Y. Suzuki, *Mater. Chem. Phys*. **17,** 87 (1987).
21. S. Yamanaka and K. Makita, *J. Porous Mater*. **1,** 29 (1995).
22. M. L. Occelli, P. A. Peaden, G. P. Ritz, P. S. Iyer, and M. Yokoyama, *Microporous Mater*. **1,** 99 (1993).
23. M. L. Occelli, *J. Mol. Catal*. **35,** 377 (1986).
24. S. Yamanaka, Y. Inoue, M. Hattori, F. Okumura, and M. Yoshikawa, *Bull. Chem. Soc. Jpn*. **65,** 2494 (1992).
25. Y. S. Han, H. Matsumoto, and S. Yamanaka, *Chem. Mater*. **9,** 2013 (1997).
26. J. Sterte, *Catal. Today* **2,** 219 (1988).
27. K. Urabe, N. Kohno, H. Sakurai, and Y. Izumi, *Adv. Mater*. **3,** 558 (1991).
28. J. Guan and T. J. Pinnavaia, *Mater. Sci. Forum* **152**/**153**, 109 (1994).
29. S. J.Gregg and K. S. W. Sing, "Adsorption, Surface Area and Porosity," 2nd ed. Academic Press, London, 1982.
30. R. S. Mikahail, S. Brunauer, and E. E. Bodor, *J. Collid. Interface Sci*. **26,** 54 (1968).
31. D. T. B. Tennakoon, J. M. Thomas, W. Jones, A. Carpenter, and R. Subramanian, *J. Chem. Soc. Faraday Trans*. **82,** 545 (1986).
32. D. T. B. Tennakoon, W. Jones, J. M. Thomas, J. H. Ballantine, and J. H. Purnell, *Solid State Ionics* **24,** 205 (1987).
33. S. Yamanaka, P. B. Malla, and S. Komarneni, *J. Collid. Interface Sci*. **134,** 51 (1990).
34. K. S. W. Sing, *Ber. Bunsen-Gesell*. **79,** 725 (1975).
35. M. S. Tzou and T. J. Pinnavaia, *Catal. Today* **2,** 243 (1988).
30. J. Bjerrum, G. Schwarzenbach, and L. G. Sillen, "Stability Constants of Metal–Ion Complexes," Spec. Publ., p. 17. Chem. Soc., London, 1964.
37. R. N. Sylva, *Rev. Pure Appl. Chem*. **22,** 115 (1972).
38. S. L. Jones, *Catal. Today* **2,** 209 (1988).